2002

Flux Recovery from Primal Hybrid Finite Element Methods

So-Hsiang Chou
Bowling Green State University, chou@bgsu.edu

Do Y. Kwak

Kwang Y. Kim

SIAM J. NUMER. ANAL.
Vol. 40, No. 2, pp. 403–415

FLUX RECOVERY FROM PRIMAL HYBRID FINITE ELEMENT METHODS*

SO-HSIANG CHOU†, DO Y. KWAK‡, AND KWANG Y. KIM‡

Abstract. A flux recovery technique is introduced and analyzed for the computed solution of the primal hybrid finite element method for second-order elliptic problems. The recovery is carried out over a single element at a time while ensuring the continuity of the flux across the interelement edges and the validity of the discrete conservation law at the element level. Our construction is general enough to cover all degrees of polynomials and grids of triangular or quadrilateral type. We illustrate the principle using the Raviart–Thomas spaces, but other well-known related function spaces such as the Brezzi–Douglas–Marini (BDM) or Brezzi–Douglas–Fortin–Marini (BDFM) space can be used as well. An extension of the technique to the nonlinear case is given. Numerical results are presented to confirm the theoretical results.

Key words. recovery technique, primal hybrid method, nonconforming method, conservative method

AMS subject classifications. 65N15, 65N30

PII. S0036142900381266

1. Introduction.

We consider the second-order elliptic boundary value problem

$$\begin{cases} -\operatorname{div}(\mathcal{K}\nabla u) = f & \text{in } \Omega, \\ u = 0 & \text{on } \partial\Omega, \end{cases} \tag{1.1}$$

where Ω is a bounded polygonal domain in $\mathbb{R}^2$ with the boundary $\partial\Omega$, and $\mathcal{K} = \mathcal{K}(\mathbf{x})$ is assumed to be symmetric and uniformly positive definite, i.e., there exist two positive constants c_1 and c_2 such that

$$c_1\xi^T\xi \le \xi^T\mathcal{K}(\mathbf{x})\xi \le c_2\xi^T\xi \qquad \forall \xi \in \mathbb{R}^2,\ \mathbf{x} \in \overline{\Omega}.$$

In many applications, it is more important to gain accurate approximation for the vector variable $\boldsymbol{\sigma} = -\mathcal{K}\nabla u$ (e.g., Darcy velocity) rather than the scalar variable u (e.g., pressure). A common way of achieving that goal is to use the mixed finite element methods, which have been a very active area of research since the late 1970s; see, for example, [4, 5, 6, 9, 20, 22]. All mixed methods have the further advantage of maintaining the discrete conservation law at the element level.

However, mixed methods lead to an indefinite symmetric algebraic system which may be hard to solve iteratively. An efficient way to solve for the mixed finite element method is to further introduce the Lagrange multipliers on the edges of the mesh to ensure the continuity of normal components of the velocity variable. This is sometimes called the mixed-hybrid method. In this fashion the velocity and the pressure finite element spaces have no continuity constraints at all, and thus both variables can be

*Received by the editors November 15, 2000; accepted for publication (in revised form) January 10, 2002; published electronically May 29, 2002.
http://www.siam.org/journals/sinum/40-2/38126.html

†Department of Mathematics and Statistics, Bowling Green State University, Bowling Green, OH (chou@bgnet.bgsu.edu). The research of this author was supported by NSF grant DMS–0074259.

‡Department of Mathematics, Korea Advanced Institute of Science and Technology, Taejon, Korea 305-701 (dykwak@math.kaist.ac.kr, kky@mathx.kaist.ac.kr). This work was supported by grant 2000-2-10300-001-5 from the Basic Research Program of the Korea Science & Engineering Foundation.

eliminated to obtain a symmetric and positive definite matrix system which involves only the Lagrange multipliers. It can be shown that this matrix system is equivalent to some nonconforming finite element method for the original problem (1.1); see, for example, [1, 2, 7]. The nonconforming method for the pressure requires fewer degrees of freedom than the mixed finite element method, and moreover, its solution can be computed by a fast solver such as multigrid algorithms (cf. [3, 8, 10, 11]). By using this nonconforming solution, the vector approximation can be obtained through a simple formula, for example, as done in [17]. The rectangular case with piecewise constant diagonal tensor was considered in [8]. For the triangular case, see [1, 2, 7, 8, 17].

Our objective in this paper is to show that similar equivalence results can be derived through the primal hybrid finite element methods for the problem (1.1) which were analyzed in [21] as a general approach of constructing nonconforming finite element approximations. We first present a technique of recovering from the primal hybrid solution an optimal flux approximation $\boldsymbol{\sigma}_h$ based on the local Raviart–Thomas spaces. Although the construction is carried out in a local manner (over a single element at a time), it is ensured that $\boldsymbol{\sigma}_h$ is continuous across the interelement boundaries and that the discrete conservation law holds locally. Also, instead of the Raviart–Thomas spaces, other mixed finite element spaces such as the Brezzi–Douglas–Marini (BDM) spaces or the Brezzi–Douglas–Fortin–Marini (BDFM) spaces can be used as well.

The main advantage of our technique is that it is general enough to cover all degrees of polynomials and all types of grids, triangular or quadrilateral. In particular, our technique can be applied to any nonconforming finite element method which can be viewed as a primal hybrid finite element method.

As good examples of how the technique can be applied, we will derive simple formulas for $\boldsymbol{\sigma}_h$ in the lowest-order cases on triangular and quadrilateral grids, which lead to the $P1$ and the rotated $Q1$ nonconforming finite element methods, respectively (see [21] or section 4).

The rest of the paper is organized as follows. In the next section the primal finite element methods are introduced for the problem (1.1). In section 3, we present a technique of flux recovery from the primal hybrid finite element methods and establish optimal error estimates for the vector approximation thus obtained, and in section 4 a detailed description of how the technique can be applied for the lowest-order elements is given. In section 5, our results are extended to nonlinear problems. Finally, in section 6, some numerical results are presented to confirm the theoretical results.

2. Primal hybrid finite element methods. In this section we give a brief description of the primal hybrid finite element method for the problem (1.1). The reader can find much more detail on this subject in [21].

Let $\mathcal{T}_h$ be a partition of Ω into triangles or convex quadrilaterals which satisfies the usual regularity assumption

$$C_1 h_T^2 \le |T| \le C_2 h_T^2 \qquad \forall T \in \mathcal{T}_h,$$

where h_T denotes the diameter of T, $|T|$ is the area of T, and $h = \max_{T\in\mathcal{T}_h} h_T$.

Denote by $\hat{T}$ a standard reference element, i.e., the unit square or the unit triangle with the vertices $\hat{\mathbf{x}}_i$'s. Then there exists a unique bijective bilinear or linear transformation $F_T : \hat{T} \to T$ such that $\mathbf{x}_i = F_T(\hat{\mathbf{x}}_i)$ for all i. We set

$$\mathcal{J}_T = \text{ Jacobian matrix of } F_T, \qquad J_T = \det \mathcal{J}_T.$$

Based on the triangulation $\mathcal{T}_h$ we define the spaces

$$X = \{v \in L^2(\Omega) : v|_T \in H^1(T) \quad \forall T \in \mathcal{T}_h\} = \prod_{T\in\mathcal{T}_h} H^1(T),$$

$$M = \Big\{\mu \in \prod_{T\in\mathcal{T}_h} H^{-1/2}(\partial T) : \text{ there exists } \boldsymbol{\tau} \in \mathbf{H}(\mathrm{div},\Omega) \text{ such that } \boldsymbol{\tau}\cdot\mathbf{n}_T = \mu \text{ on } \partial T, \qquad \forall T \in \mathcal{T}_h\Big\},$$

where $\mathbf{n}_T$ is the unit outward normal along ∂T. Let $|\cdot|_{m,\Omega}$ and $\|\cdot\|_{m,\Omega}$ denote the usual seminorm and norm, respectively, on the Sobolev space $H^m(\Omega)$. We define the mesh-dependent norms

$$|||v|||_X = \left(\sum_{T\in\mathcal{T}_h} |||v|||_{1,T}^2\right)^{1/2}, \qquad v \in X,$$

$$\|\mu\|_h = \left(\sum_{T\in\mathcal{T}_h} h_T\|\mu\|_{0,\partial T}^2\right)^{1/2}, \qquad \mu \in \prod_{T\in\mathcal{T}_h} L^2(\partial T),$$

where

$$|||v|||_{1,T}^2 = |v|_{1,T}^2 + h_T^{-2}\|v\|_{0,T}^2.$$

Now the primal hybrid formulation for the problem (1.1) is given as follows: find a pair $(u,\lambda) \in X \times M$ such that

$$a(u,v) + b(v,\lambda) = (f,v) \qquad \forall v \in X, \tag{2.1a}$$

$$b(u,\mu) = 0 \qquad \forall \mu \in M, \tag{2.1b}$$

where

$$a(u,v) = \sum_{T\in\mathcal{T}_h} \int_T \mathcal{K}\nabla u\cdot\nabla v\,dx, \qquad b(v,\mu) = \sum_{T\in\mathcal{T}_h} \int_{\partial T} v\mu\,ds, \tag{2.2}$$

$$(f,v) = \int_\Omega fv\,dx. \tag{2.3}$$

It was shown in [21] that u belongs to $H_0^1(\Omega)$ and is the unique solution of the standard weak formulation

$$\int_\Omega \mathcal{K}\nabla u\cdot\nabla v\,dx = \int_\Omega fv\,dx, \qquad v \in H_0^1(\Omega),$$

and that

$$\lambda = -\mathcal{K}\nabla u\cdot\mathbf{n}_T \ \text{ on } \partial T \qquad \forall T \in \mathcal{T}_h. \tag{2.4}$$

We use the standard notation for the spaces of polynomials, i.e., $P_r(T)$ denotes the space of polynomials on T of total degrees at most r, and $Q_{r,s}(T)$ denotes the space of polynomials on T of degrees at most r and s in x and y, respectively. We also set $Q_r(T) = Q_{r,r}(T)$. On any element T we define

$$R_r(T) = \begin{cases} P_r(T) & \text{if } T \text{ is a triangle,} \\ Q_r(\hat{T})\circ F_T^{-1} & \text{if } T \text{ is a quadrilateral} \end{cases}$$

and

$$S_r(\partial T) = \{\mu \in L^2(\partial T) : \mu|_e \in P_r(e) \qquad \forall e \text{ edges of } T\}.$$

In order to discretize the primal hybrid formulation (2.1), we introduce a finite-dimensional subspace $\hat{X}$ of $H^1(\hat{T})$ such that $R_k(\hat{T}) \subset \hat{X}$ for some $k \geq 1$. Then we define a pair $X_h \times M_h$ of finite element spaces on $\mathcal{T}_h$ by

$$X_h = \{v \in X : v|_T \in X_h(T) \qquad \forall T \in \mathcal{T}_h\}, \tag{2.5}$$

$$M_h = \left\{ \mu \in \prod_{T \in \mathcal{T}_h} S_{k-1}(\partial T) : \mu|_{\partial T_1} + \mu|_{\partial T_2} = 0 \text{ on } \partial T_1 \cap \partial T_2 \right. \\ \left. \text{if } T_1 \text{ and } T_2 \text{ are adjacent elements} \right\}, \tag{2.6}$$

where we set $X_h(T) = \{\hat{v} \circ F_T^{-1} : \hat{v} \in \hat{X}\}$.

Now the primal hybrid finite element method is defined as follows: find a pair $(u_h, \lambda_h) \in X_h \times M_h$ such that

$$a(u_h, v) + b(v, \lambda_h) = (f, v) \qquad \forall v \in X_h, \tag{2.7a}$$

$$b(u_h, \mu) = 0 \qquad \forall \mu \in M_h. \tag{2.7b}$$

Examples for the space $\hat{X}$ are given in [21] for all $k \geq 1$ which ensures the existence and uniqueness of a solution (u_h, λ_h) for the system (2.7) and satisfy the following optimal error estimates (cf. [15, 21]).

THEOREM 2.1. *For $u \in H^{k+1}(\Omega)$ we have*

$$|||u - u_h|||_X + \|\lambda - \lambda_h\|_h \leq Ch^k |u|_{k+1}.$$

The following observation is crucial to decouple the mixed system (2.7): u_h is the solution of the *nonconforming* finite element method

$$a(u_h, v) = (f, v), \qquad v \in V_h, \tag{2.8}$$

where

$$V_h = \{v \in X_h : b(v, \mu) = 0 \qquad \forall \mu \in M_h\}. \tag{2.9}$$

This implies that we may compute u_h directly from (2.8) and then compute λ_h from u_h locally by (2.7a), which reduces to

$$\int_{\partial T} v\lambda_h \, ds = \int_T fv \, dx - \int_T \mathcal{K}\nabla u_h \cdot \nabla v \, dx, \qquad v \in X_h(T). \tag{2.10}$$

Thus, the Lagrange multiplier λ_h may be interpreted as the (weak) *local residuals* of the nonconforming approximation u_h.

3. Flux recovery technique. To begin with, we define the Raviart–Thomas space of index $r \geq 0$ on $\mathcal{T}_h$ as follows:

$$RT_r = \{\boldsymbol{\tau} \in \mathbf{H}(\mathrm{div}, \Omega) : \boldsymbol{\tau}|_T \in RT_r(T)\},$$

where the local space $RT_r(T)$ is defined as

$$RT_r(T) = \{\mathcal{P}_T\hat{\boldsymbol{\tau}} : \hat{\boldsymbol{\tau}} \in (R_r(\hat{T}))^2 + (x,y)R_r(\hat{T})\},$$

and $\mathcal{P}_T\hat{\boldsymbol{\tau}} = J_T^{-1}\mathcal{J}_T\hat{\boldsymbol{\tau}} \circ F_T^{-1}$. We also set for $r \geq 1$

$$\boldsymbol{\Psi}_r(T) = \begin{cases} (P_{r-1}(T))^2 & \text{if } T \text{ is a triangle,} \\ \{\mathcal{J}_T^{-t}\hat{\boldsymbol{\tau}} \circ F_T^{-1} : \hat{\boldsymbol{\tau}} \in Q_{r-1,r}(\hat{T}) \times Q_{r,r-1}(\hat{T})\} & \text{if } T \text{ is a quadrilateral.} \end{cases}$$

Let us point out that if T is a rectangle, then

$$\boldsymbol{\Psi}_r(T) = Q_{r-1,r}(T) \times Q_{r,r-1}(T).$$

Now we present a technique of recovering an optimal vector approximation. Once the solution (u_h, λ_h) of the system (2.7) is computed, one can construct a unique $\boldsymbol{\sigma}_h \in RT_{k-1}(T)$ on each $T \in \mathcal{T}_h$:

$$\boldsymbol{\sigma}_h \cdot \mathbf{n}_T = \lambda_h \quad \text{on } \partial T, \tag{3.1a}$$

$$\int_T (\boldsymbol{\sigma}_h + \mathcal{K}\nabla u_h) \cdot \boldsymbol{\tau}\, dx = 0, \quad \boldsymbol{\tau} \in \boldsymbol{\Psi}_{k-1}(T) \quad (k \geq 2) \tag{3.1b}$$

(cf. [6, 20, 22]). By construction we immediately obtain the following two propositions.

PROPOSITION 3.1. *The normal components of $\boldsymbol{\sigma}_h$ are continuous across the interelement boundaries, i.e., we have $\boldsymbol{\sigma}_h \in RT_{k-1}$.*

Proof. This is a direct consequence of (3.1a). ∎

PROPOSITION 3.2. *We have for all $v \in R_{k-1}(T)$*

$$\int_T \operatorname{div} \boldsymbol{\sigma}_h\, v\, dx = \int_T f v\, dx.$$

This implies that the discrete conservation law holds locally.

Proof. By using (3.1a) and Green's theorem, (2.7a) becomes

$$\int_T (\boldsymbol{\sigma}_h + \mathcal{K}\nabla u_h) \cdot \nabla v\, dx + \int_T \operatorname{div} \boldsymbol{\sigma}_h\, v\, dx = \int_T f v\, dx \qquad \forall v \in X_h(T). \tag{3.2}$$

There is nothing to be done for $k = 1$, since $\nabla v = 0$ for $v \in R_0(T)$. For $k \geq 2$ we have $\nabla v \in \boldsymbol{\Psi}_{k-1}(T)$ for $v \in R_{k-1}(T)$, which proves the desired result by (3.1b). ∎

Remark 3.1. We could use other mixed finite elements instead of RT_{k-1}. For example, when one wants to use the $BDM_{k-1}(T)$ space on a triangle T ($k \geq 2$), (3.1) is replaced by

$$\boldsymbol{\sigma}_h \cdot \mathbf{n}_T = \lambda_h \quad \text{on } \partial T, \tag{3.3a}$$

$$\int_T (\boldsymbol{\sigma}_h + \mathcal{K}\nabla u_h) \cdot \nabla v\, dx = 0, \quad v \in P_{k-2}(T), \tag{3.3b}$$

$$\int_T (\boldsymbol{\sigma}_h + \mathcal{K}\nabla u_h) \cdot \operatorname{curl}(b_T v)\, dx = 0, \quad v \in P_{k-3}(T) \quad (k \geq 3), \tag{3.3c}$$

where b_T is the cubic bubble function on T. If the space $\hat{X}$ contains only $P_k(\hat{T})$ on a quadrilateral T, one may use the $BDFM_k(T)$ space, in which case (3.1) is replaced by

$$\boldsymbol{\sigma}_h \cdot \mathbf{n}_T = \lambda_h \quad \text{on } \partial T, \tag{3.4a}$$

$$\int_T (\boldsymbol{\sigma}_h + \mathcal{K}\nabla u_h) \cdot \boldsymbol{\tau}\, dx = 0, \quad \boldsymbol{\tau} \in \boldsymbol{\Psi}_{k-1}(T) \quad (k \geq 2), \tag{3.4b}$$

where we set

$$\boldsymbol{\Psi}_r(T) = \{\mathcal{J}_T^{-t}\hat{\boldsymbol{\tau}} \circ F_T^{-1} : \hat{\boldsymbol{\tau}} \in (P_{r-1}(\hat{T}))^2\}.$$

For a review of the degrees of freedom (3.3) and (3.4), we refer to [4, 5, 6].

Before going to an error estimate, we prove the following key lemma.

LEMMA 3.3. *Given $\beta \in L^2(\partial T)$ and $\mathbf{q} \in (L^2(T))^2$, let $\boldsymbol{\xi}_h \in RT_r(T)$ satisfy*

$$\int_{\partial T} \boldsymbol{\xi}_h \cdot \mathbf{n}_T\, \mu\, ds = \int_{\partial T} \beta\mu\, ds \qquad \forall \mu \in S_r(\partial T),$$

$$\int_T \boldsymbol{\xi}_h \cdot \boldsymbol{\tau}\, dx = \int_T \mathbf{q} \cdot \boldsymbol{\tau}\, dx \qquad \forall \boldsymbol{\tau} \in \boldsymbol{\Psi}_r(T) \quad (r \geq 1).$$

Then we obtain

$$\|\boldsymbol{\xi}_h\|_{0,T} \leq C(\|\mathbf{q}\|_{0,T} + h_T^{1/2}\|\beta\|_{0,\partial T}).$$

Proof. By considering the L^2 projections, we may assume that $\beta \in S_r(\partial T)$ and $\mathbf{q} \in RT_r(T)$. Then the proof is done by using a simple scaling argument [2, 6]. ∎

Now we derive an error estimate for the vector approximation $\boldsymbol{\sigma}_h$ constructed by (3.1). It is well known (see, e.g., [6, 20, 22, 23]) that the Raviart–Thomas projection $\Pi_h : (H^1(\Omega))^2 \to RT_r$ can be defined by

$$\int_{\partial T} \Pi_h\boldsymbol{\sigma} \cdot \mathbf{n}\, \mu\, ds = \int_{\partial T} \boldsymbol{\sigma} \cdot \mathbf{n}\, \mu\, ds, \qquad \mu \in S_r(\partial T), \tag{3.5}$$

$$\int_T \Pi_h\boldsymbol{\sigma} \cdot \boldsymbol{\tau}\, dx = \int_T \boldsymbol{\sigma} \cdot \boldsymbol{\tau}\, dx, \qquad \boldsymbol{\tau} \in \boldsymbol{\Psi}_r(T), \tag{3.6}$$

possessing the following approximation properties:

$$\|\boldsymbol{\sigma} - \Pi_h\boldsymbol{\sigma}\|_0 \leq Ch^l\, \|\boldsymbol{\sigma}\|_l, \qquad 1 \leq l \leq r+1,$$

for all $\boldsymbol{\sigma} \in (H^l(\Omega))^2$, and

$$\|\operatorname{div}(\boldsymbol{\sigma} - \Pi_h\boldsymbol{\sigma})\|_0 \leq Ch^l\, \|\operatorname{div}\boldsymbol{\sigma}\|_l, \qquad 0 \leq l \leq r+1,$$

for all $\boldsymbol{\sigma} \in (H^l(\Omega))^2$ with $\operatorname{div}\boldsymbol{\sigma} \in H^l(\Omega)$.

THEOREM 3.4. *Let $\boldsymbol{\sigma} = -\mathcal{K}\nabla u$. Then we have for $u \in H^{k+1}(\Omega)$*

$$\|\boldsymbol{\sigma} - \boldsymbol{\sigma}_h\|_0 \leq Ch^k(|\boldsymbol{\sigma}|_k + |u|_{k+1}).$$

Proof. It suffices to prove that

$$\|\Pi_h\boldsymbol{\sigma} - \boldsymbol{\sigma}_h\|_{0,T} \leq Ch^k(|\boldsymbol{\sigma}|_k + |u|_{k+1}).$$

From (3.5) and (3.6) it follows that

$$\int_{\partial T}(\Pi_h\boldsymbol{\sigma}-\boldsymbol{\sigma}_h)\cdot\mathbf{n}_T\,\mu\,ds=\int_{\partial T}(\lambda-\lambda_h)\mu\,ds,\quad \mu\in S_{k-1}(\partial T),$$
$$\int_T(\Pi_h\boldsymbol{\sigma}-\boldsymbol{\sigma}_h)\cdot\boldsymbol{\tau}\,dx=-\int_T\mathcal{K}\nabla(u-u_h)\cdot\boldsymbol{\tau}\,dx,\quad \boldsymbol{\tau}\in\boldsymbol{\Psi}_{k-1}(T)\quad (k\geq 2).$$

By applying Lemma 3.3 and then Theorem 2.1, we obtain

$$\begin{aligned}\|\Pi_h\boldsymbol{\sigma}-\boldsymbol{\sigma}_h\|_{0,T}&\leq C(|u-u_h|_{1,T}+h_T^{1/2}\|\lambda-\lambda_h\|_{0,\partial T})\\&\leq Ch^k(|\boldsymbol{\sigma}|_k+|u|_{k+1}).\end{aligned}$$

This completes the proof. ∎

4. Examples. In this section $\bar{f}$ indicates the piecewise constant average of f on $\mathcal{T}_h$, i.e.,

$$\bar{f}|_T=\frac{1}{|T|}\int_T f\,dx.$$

4.1. *P*1 nonconforming method. Let $\mathcal{T}_h$ be composed of triangles. We consider the lowest-order element, i.e., $k=1$:

$$X_h(T)=P_1(T),\qquad M_h=\prod_{T\in\mathcal{T}_h}S_0(\partial T)\bigcap M.$$

Then it is easy to see that V_h (defined by (2.9)) is the $P1$ nonconforming finite element space.

Let T be an arbitrary element of $\mathcal{T}_h$ with the edges e_1,e_2,e_3 and the barycenter $\mathbf{x}_T$, and let $\phi_i\in X_h(T)$ be the basis function associated with the edge e_i, namely, $\frac{1}{|e_i|}\int_{e_i}\phi_j\,ds=\delta_{ij}$. Then $\lambda_h|_{e_i}$ is given by (see (2.10))

$$\lambda_h|_{e_i}=\frac{1}{|e_i|}\left(\int_T f\phi_i\,dx-\int_T\mathcal{K}\nabla u_h\cdot\nabla\phi_i\,dx\right).$$

Using the formula $\nabla\phi_i=\frac{\mathbf{n}_i|e_i|}{|T|}$ results in

$$\lambda_h|_{e_i}=-\bar{\mathcal{K}}\nabla u_h\cdot\mathbf{n}_i+\frac{1}{|e_i|}\int_T f\phi_i\,dx.$$

By comparing the normal components $\boldsymbol{\sigma}_h\cdot\mathbf{n}_i$ for each i, one can show that the vector $\boldsymbol{\sigma}_h$ constructed by (3.1) is identical to the one given in [13]:

$$\boldsymbol{\sigma}_h=-\bar{\mathcal{K}}\nabla u_h+\frac{\bar{f}}{2}(\mathbf{x}-\mathbf{x}_T)+\mathbf{C}_T,\tag{4.1}$$

where $\mathbf{C}_T$ is determined by any two of the three equations

$$|e_i|\mathbf{n}_i\cdot\mathbf{C}_T=\int_T f\phi_i\,dx-\frac{|T|}{3}\bar{f},\qquad i=1,2,3.$$

In particular, when f is a constant on T, we obtain $\mathbf{C}_T=0$ and

$$\boldsymbol{\sigma}_h|_T=-\bar{\mathcal{K}}\nabla u_h|_T+\frac{f}{2}(\mathbf{x}-\mathbf{x}_T),\tag{4.2}$$

which is the formula obtained by Marini [17].

Remark 4.1. It is straightforward to extend the above results to higher-order elements of odd degrees $k \geq 3$:

$$X_h(T) = P_k(T), \qquad M_h = \prod_{T \in \mathcal{T}_h} S_{k-1}(\partial T) \bigcap M.$$

Once u_h is computed, λ_h can be computed at k Gauss–Legendre points on each edge by using the basis functions associated with these points.

Now let us consider the primal hybrid finite element method with the right-hand side f replaced by $\bar{f}$. By Proposition 3.2 we then have

$$\int_T \operatorname{div} \boldsymbol{\sigma}_h \, dx = \int_T \bar{f} \, dx, \tag{4.3a}$$

or $\operatorname{div} \boldsymbol{\sigma}_h = \bar{f}$. This, together with (3.2), implies that

$$\int_T (\boldsymbol{\sigma}_h + \mathcal{K} \nabla u_h) \, dx = 0. \tag{4.3b}$$

The equations (4.3a)–(4.3b) form the finite volume box method introduced by Courbet and Croisille [14]. Thus the primal hybrid finite element method along with our technique of flux recovery provide an alternative approach to the finite volume box method. A different approach is given in [13]; see also [12].

4.2. Rotated $Q1$ nonconforming method. Let $\mathcal{T}_h$ be composed of quadrilaterals, and

$$\hat{X} = \operatorname{span}\{1, \hat{x}, \hat{y}, \hat{x}^2 - \hat{y}^2\}, \qquad M_h = \prod_{T \in \mathcal{T}_h} S_0(\partial T) \bigcap M.$$

Then it is easy to see that V_h is the *parametric* rotated $Q1$ nonconforming finite element space introduced by Rannacher and Turek [19]. One could use the nonparametric version as well which, on rectangular grids, is given by

$$X_h(T) = \operatorname{span}\{1, x, y, x^2 - y^2\}, \qquad M_h = \prod_{T \in \mathcal{T}_h} S_0(\partial T) \bigcap M.$$

As in the $P1$ nonconforming method, $\lambda_h|_{e_i}$ is given by

$$\lambda_h|_{e_i} = \frac{1}{|e_i|} \left(\int_T f \phi_i \, dx - \int_T \nabla u_h \cdot \nabla \phi_i \, dx \right),$$

where $\phi_i \in X_h(T)$ is the basis function associated with the edge e_i.

Now we derive a simple formula for $\boldsymbol{\sigma}_h$ for the nonparametric version on rectangular grids. Suppose that f is piecewise constant. Then we obtain $\operatorname{div} \boldsymbol{\sigma}_h = f$ and

$$\int_T (\boldsymbol{\sigma}_h + \mathcal{K} \nabla u_h) \cdot \nabla v \, dx = 0 \qquad \forall v \in X_h(T). \tag{4.4}$$

Let us decompose $\boldsymbol{\sigma}_h|_T$ into

$$\boldsymbol{\sigma}_h|_T = \boldsymbol{\sigma}_{h,0}|_T + a_T(h_{T_y}^2 (x - x_T), h_{T_x}^2 (y - y_T)),$$

where $\boldsymbol{\sigma}_{h,0}|_T$ belongs to

$$\nabla X_h(T) = \{(a + bx, c - by) : a, b, c \in \mathbb{R}\},$$

and h_{T_x} and h_{T_y} are the width and the height of T, respectively. Since we have $\operatorname{div} \boldsymbol{\sigma}_{h,0}|_T = 0$, it follows that

$$a_T = \frac{f|_T}{h_{T_x}^2 + h_{T_y}^2}.$$

Now, by means of the orthogonality relation

$$\int_T (h_{T_y}^2(x - x_T), h_{T_x}^2(y - y_T)) \cdot \nabla v \, dx = 0, \qquad v \in X_h(T),$$

it is easy to see from (4.4) that

$$\boldsymbol{\sigma}_{h,0} = -P_0(\mathcal{K}\nabla u_h), \tag{4.5}$$

where P_0 is the L^2 projection which locally maps onto the space $\nabla X_h(T)$. Combining the results obtained thus far, we obtain

$$\boldsymbol{\sigma}_h|_T = -P_0(\mathcal{K}\nabla u_h)|_T + \frac{f|_T}{h_{T_x}^2 + h_{T_y}^2}(h_{T_y}^2(x - x_T), h_{T_x}^2(y - y_T)). \tag{4.6}$$

Remark 4.2. Similar results using the lowest-order rectangular Raviart–Thomas mixed finite element method can be found in [1, 8]. Our results show the primal hybrid approach provides a clear way of constructing the vector approximation from the Q_1 nonconforming solution.

5. Extension to nonlinear problems. The previous results can be extended to the nonlinear second-order elliptic boundary value problem

$$\begin{cases} -\operatorname{div} \mathbf{a}(u, \nabla u) = f & \text{in } \Omega, \\ u = 0 & \text{on } \partial\Omega. \end{cases} \tag{5.1}$$

The primal hybrid formulation is to find a pair $(u, \lambda) \in X \times M$ such that

$$a(u, v) + b(v, \lambda) = (f, v) \qquad \forall v \in X, \tag{5.2a}$$

$$b(u, v) = 0 \qquad \forall \mu \in M, \tag{5.2b}$$

where

$$a(u, v) = \sum_{T \in \mathcal{T}_h} \int_T \mathbf{a}(u, \nabla u) \cdot \nabla v \, dx. \tag{5.3}$$

Analysis of the primal hybrid finite element methods for this nonlinear problem is given in [18] for $k \geq 2$.

The previous technique of recovering a vector approximation can be applied as well. After computing the primal hybrid solution (u_h, λ_h), one constructs a unique $\boldsymbol{\sigma}_h \in RT_{k-1}(T)$ on each $T \in \mathcal{T}_h$ by

$$\boldsymbol{\sigma}_h \cdot \mathbf{n}_T = \lambda_h \quad \text{on } \partial T, \tag{5.4a}$$

$$\int_T [\boldsymbol{\sigma}_h + \mathbf{a}(u_h, \nabla u_h)] \cdot \boldsymbol{\tau} \, dx = 0, \quad \boldsymbol{\tau} \in \boldsymbol{\Psi}_{k-1}(T) \quad (k \geq 2). \tag{5.4b}$$

Setting $\boldsymbol{\sigma} = -\mathbf{a}(u, \nabla u)$, we can derive the bound for $\|\boldsymbol{\sigma} - \boldsymbol{\sigma}_h\|_0$ in the same way as before. By applying Lemma 3.3 to the error equations

$$\int_{\partial T} (\Pi_h \boldsymbol{\sigma} - \boldsymbol{\sigma}_h) \cdot \mathbf{n}_T \, \mu \, ds = \int_{\partial T} (\lambda - \lambda_h) \mu \, ds, \quad \mu \in S_{k-1}(\partial T),$$
$$\int_T (\Pi_h \boldsymbol{\sigma} - \boldsymbol{\sigma}_h) \cdot \boldsymbol{\tau} \, dx = -\int_T [\mathbf{a}(u, \nabla u) - \mathbf{a}(u_h, \nabla u_h)] \cdot \boldsymbol{\tau} \, dx,$$
$$\boldsymbol{\tau} \in \boldsymbol{\Psi}_{k-1}(T) \quad (k \geq 2),$$

we obtain

$$\|\Pi_h \boldsymbol{\sigma} - \boldsymbol{\sigma}_h\|_{0,T} \leq C(\|\mathbf{a}(u, \nabla u) - \mathbf{a}(u_h, \nabla u_h)\|_{0,T} + h_T^{1/2} \|\lambda - \lambda_h\|_{0,\partial T}).$$

Note that if $\mathbf{a}$ has bounded derivatives, then there exists a constant $C > 0$ independent of h such that

$$|\mathbf{a}(u, \nabla u) - \mathbf{a}(u_h, \nabla u_h)| \leq C(|u - u_h| + |\nabla(u - u_h)|),$$

which implies that

$$\|\mathbf{a}(u, \nabla u) - \mathbf{a}(u_h, \nabla u_h)\|_{0,T} \leq C \|u - u_h\|_{1,T}.$$

Thus it follows by Theorem 2.1 that

$$\|\Pi_h \boldsymbol{\sigma} - \boldsymbol{\sigma}_h\|_{0,T} \leq C h^k (|\boldsymbol{\sigma}|_k + |u|_{k+1}).$$

THEOREM 5.1. *We have for* $u \in H^{k+1}(\Omega)$

$$\|\boldsymbol{\sigma} - \boldsymbol{\sigma}_h\|_0 \leq C h^k (|\boldsymbol{\sigma}|_k + |u|_{k+1}).$$

6. Numerical results. To confirm the theoretical results established in the previous sections, numerical experiments are carried out on the unit square $\Omega = (0, 1)^2$ for three test problems. The first problem has a discontinuous tensor coefficient, and the second one has a smooth coefficient, but its solution has a very weak "layer" near the right boundary. Finally the third problem is taken from [16]. For numerical results on triangular grids, we refer to [13].

Errors for the velocity and the pressure approximations are computed in the discrete L^2 norms

$$\|\boldsymbol{\sigma} - \boldsymbol{\sigma}_h\|_{0,h}^2 = \sum_{T \in \mathcal{T}_h} \sum_{e \in \partial T} \left[\int_e (\boldsymbol{\sigma} - \boldsymbol{\sigma}_h) \cdot \mathbf{n} \, ds \right]^2, \tag{6.1}$$

$$\|u - u_h\|_{0,h}^2 = \sum_{T \in \mathcal{T}_h} \int_T (u - u_h)^2 \, dxdy, \tag{6.2}$$

where the integrals are evaluated by the midpoint rule, i.e., if S denotes an edge e or an area T, then we evaluate $\int_S g$ by $|S| \times g(\mathbf{x}_S)$, where $\mathbf{x}_S$ is the mass center of S. All the results below show second-order convergence in the velocity. They are tabulated as Tables 6.1–6.3.

PROBLEM 1.

$$\mathcal{K} = \begin{pmatrix} 10^4 & 0 \\ 0 & 1 \end{pmatrix} \text{ for } 0 < x < .5, \qquad \begin{pmatrix} 1 & 0 \\ 0 & 2 \end{pmatrix} \text{ for } .5 < x < 1,$$

TABLE 6.1
Problem 1. *Discontinuous tensor coefficients.*

h	$\|\mathfrak{E} - \mathfrak{E}_h\|_{0,h}$	$\|u - u_h\|_{0,h}$
1/8	2.58135e-1	5.60052e-4
1/16	2.64380e-1	1.39916e-4
1/32	7.91115e-2	3.49786e-5
1/64	1.97629e-2	8.74365e-6
1/128	4.93600e-3	2.18584e-6

TABLE 6.2
Problem 2. *Weak layer at the right boundary.*

h	$\|\mathfrak{E} - \mathfrak{E}_h\|_{0,h}$	$\|u - u_h\|_{0,h}$
1/8	9.30579e-2	8.34233e-2
1/16	2.67894e-2	2.21723e-2
1/32	7.01984e-3	5.63162e-3
1/64	1.77762e-3	1.41354e-3
1/128	4.45865e-4	3.53740e-4

TABLE 6.3
Problem 3. *Distorted grids,* $\beta = 60°, \theta = 45°$.

Grid size	$\|\mathfrak{E} - \mathfrak{E}_h\|_{0,h}$	$\|u - u_h\|_{0,h}$
8×8	2.0878e-1	4.1977e-2
16×16	5.2684e-2	1.0989e-2
32×32	1.3526e-2	2.7816e-3
64×64	3.4843e-3	6.9757e-4
128×128	8.9701e-4	1.7453e-4

and

$$u(x, y) = x(1 - x)y(1 - y).$$

The domain Ω *is partition into the squares of size* h. *By simple calculations it is easy to see that the velocity* $\boldsymbol{\sigma} = -\mathcal{K}\nabla u$ *has continuous normal components across the line of discontinuity* $x = 1/2$. *We use the parametric rotated* $Q1$ *nonconforming method for this problem.*

PROBLEM 2. *In this problem we let* $\mathcal{K} = I$, *the identity matrix. The exact solution is*

$$u(x, y) = x(1 - x)y(1 - y)\exp(5x),$$

which has a boundary layer. We use rectangular grids.

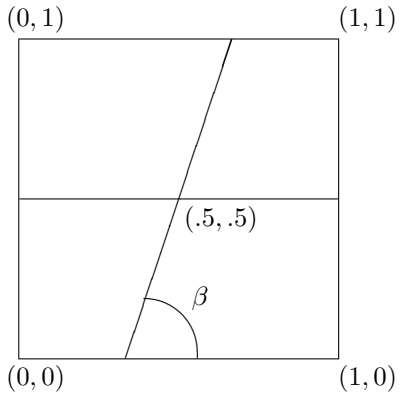

FIG. 6.1. *Distorted grids for Problem* 3.

PROBLEM 3.

$$\mathcal{K} = \begin{pmatrix} \cos\theta & \sin\theta \\ -\sin\theta & \cos\theta \end{pmatrix} \begin{pmatrix} 1 & 0 \\ 0 & 0.01 \end{pmatrix} \begin{pmatrix} \cos\theta & -\sin\theta \\ \sin\theta & \cos\theta \end{pmatrix},$$

and $u(x, y) = \cos(\pi x)\cos(2\pi y)$. *The grids are obtained through successive refinements of the initial grid shown in Figure* 6.1. *The refinement is done by connecting the midpoints of opposite edges of every quadrilateral. We use the parametric rotated* $Q1$ *nonconforming method for this problem.*

REFERENCES

[1] T. ARBOGAST AND Z. CHEN, *On the implementation of mixed methods as nonconforming methods for second order elliptic problems*, Math. Comp., 66 (1997), pp. 85–104.

[2] D. N. ARNOLD AND F. BREZZI, *Mixed and nonconforming finite element methods: Implementation, postprocessing and error estimates*, RAIRO Modél. Math. Anal. Numér., 19 (1985), pp. 7–32.

[3] S. C. BRENNER, *An optimal order multigrid for* $P1$ *nonconforming finite elements*, Math. Comp., 52 (1989), pp. 1–15.

[4] F. BREZZI, J. DOUGLAS, M. FORTIN, AND L. MARINI, *Efficient rectangular mixed finite elements in two and three variables*, RAIRO Modél. Math. Anal. Numér., 21 (1987), pp. 581–604.

[5] F. BREZZI, J. DOUGLAS, AND L. MARINI, *Two families of mixed finite elements for second order elliptic problems*, Numer. Math., 47 (1985), pp. 217–235.

[6] F. BREZZI AND M. FORTIN, *Mixed and Hybrid Finite Element Methods*, Springer-Verlag, New-York, 1991.

[7] Z. CHEN, *Analysis of mixed methods using conforming and nonconforming finite element methods*, RAIRO Modél. Math. Anal. Numér., 27 (1993), pp. 9–34.

[8] Z. CHEN, *Equivalence between and multigrid algorithms for nonconforming and mixed methods for second-order elliptic problems*, East-West J. Numer. Math., 4 (1996), pp. 1–33.

[9] Z. CHEN AND J. DOUGLAS, JR., *Prismatic mixed finite elements for second order elliptic problems*, Calcolo, 26 (1989), pp. 135–148.

[10] Z. CHEN AND D. Y. KWAK, *Convergence of multigrid methods for nonconforming finite elements without regularity assumptions*, Comput. Appl. Math., 17 (1998), pp. 283–302.

[11] Z. CHEN AND P. OSWALD, *Multigrid and multilevel methods for nonconforming* $Q1$ *elements*, Math. Comp., 67 (1998), pp. 667–693.

[12] S. H. CHOU, D. Y. KWAK, AND K. Y. KIM, *Mixed finite volume methods on non-staggered quadrilateral grids for elliptic problems*, Math. Comp., to appear.

[13] S.-H. CHOU AND S. TANG, *Conservative* $P1$ *conforming and nonconforming Galerkin FEMs: Effective flux evaluation via a nonmixed method approach*, SIAM J. Numer. Anal., 38 (2000), pp. 660–680.

[14] B. Courbet and J. P. Croisille, *Finite volume box schemes on triangular meshes*, RAIRO Modél. Math. Anal. Numér., 32 (1998), pp. 631–649.

[15] J. Douglas, C. P. Gupta, and G. Y. Li, *Global estimates for a primal hybrid finite element method for second order elliptic problems in the plane*, Mat. Apl. Comput., 2 (1983), pp. 273–283.

[16] J. E. Jones, *A Mixed Finite Volume Element Method for Accurate Computation of Fluid Velocities in Porous Media*, Ph.D. thesis, University of Colorado at Denver, Denver, CO, 1995.

[17] L. D. Marini, *An inexpensive method for the evaluation of the solution of the lowest order Raviart-Thomas mixed method*, SIAM J. Numer. Anal., 22 (1985), pp. 493–496.

[18] E. J. Park, *A primal hybrid finite element method for a strongly nonlinear second-order elliptic problem*, Numer. Methods Partial Differential Equations, 11 (1995), pp. 61–75.

[19] R. Rannacher and S. Turek, *Simple nonconforming quadrilateral Stokes element*, Numer. Methods Partial Differential Equations, 8 (1992), pp. 97–111.

[20] P. A. Raviart and J. M. Thomas, *A mixed finite element method for 2nd order elliptic problems*, in *Proceedings of the Conference on Mathematical Aspects of Finite Element Methods*, Lecture Notes in Math. 606, Springer-Verlag, Berlin, 1977, pp. 292–315.

[21] P. A. Raviart and J. M. Thomas, *Primal hybrid finite element methods for 2nd order elliptic equations*, Math. Comp., 31 (1977), pp. 391–413.

[22] J. E. Roberts and J. M. Thomas, *Mixed and hybrid methods*, in Handb. Numer. Anal., Vol. II, North-Holland, Amsterdam, 1991, pp. 523–639.

[23] J. Wang and T. Mathew, *Mixed finite element methods over quadrilaterals*, in the Proceedings of the Third International Conference on Advances in Numerical Methods and Applications, I. T. Dimov, Bl. Sendov, and P. Vassilevski, eds., World Scientific, Singapore, 1994, pp. 203–214.